ASTRONOMY & ASTROPHYSICS
SUPPLEMENT SERIES

JULY 1983, PAGE 57

Astron. Astrophys. Suppl. Ser. **53**, 57-70 (1983)

Medium size radio continuum loops and their association with HI shells

Y. Sofue ([1]) and N. Nakai ([2])

([1]) Nobeyama Radio Observatory, Tokyo Astronomical Observatories, University of Tokyo, Nobeyama, Minamisaku, 384-13 Nagano, Japan
([2]) Department of Astronomy, University of Tokyo, Yayoi-cho, Bunkyo-ku, 113 Tokyo, Japan

Received November 11, 1982, accepted January 25, 1983

Summary. — Radio continuum survey data at 408 and 820 MHz are examined in order to find very old supernova remnants, which might be hidden in the complicated background radio emission of the Galaxy. A method to substract large-scale background structures is applied so that structures of scale-sizes less than 4 degrees are abstracted. Among many loop-like features five loops of diameters 3-10 degrees are found to be associated with HI shells. They may be extremely old ($\sim 10^6$ yrs) SNRs at distances less than $\sim$ 1 kpc of the sun.

Key words : HI shell — interstellar gas — supernova remnants.

1. Introduction.

A supernova remnant (SNR) expands until the velocity of the expansion decreases down to the sound velocity of the interstellar medium. However, before they evolve up to their oldest ages, most of the SNR will fade away by merging into the interstellar medium through interactions with the interstellar turbulence and collisions among themselves. Only those exploded at very high altitudes from the galactic plane, where the frequency of SN explosions is rare compared to the near-plane region, may survive until their oldest ages. Among them those in the solar neighbourhood could be identified in regions of the sky at high galactic latitudes as very faint radio continuum loops.

Such old SNRs may be associated with neutral hydrogen shells as expected from the snow-plough effect. Heiles (1979) and Hu (1981) have found a number of large-diameter HI shells in their 21-cm line survey data. Heiles (1979) suggests that the shells may be due to some kind of explosive phenomena occurred in the interstellar gas, possibly due to supernovae. If the HI shells are due to SNR, they might be associated with nonthermal radio continuum loops.

In the present paper, we search for faint loop structures on the sky in the radio continuum emissions at 408 and 820 MHz. We also examine the relationship between the radio loops and HI shells.

Send offprint requests to : Y. Sofue.

2. Radio continuum loops.

2.1 THE DATA AND THE « BACKGROUND FILTERING (BGF) » METHOD. — The data of the radio continuum emission we use here are taken from the Bonn 408 MHz survey (Haslam *et al.*, 1974), Jodrell Bank 408 MHz survey (Haslam *et al.*, 1970) and Leiden 820 MHz survey (Berkhuijsen, 1972) which are available in the form of a magnetic tape.

In order to find faint loop structures in the background radio continuum emission, we apply the « background filtering » method (BGF) to the data. The method has been proposed by Sofue and Reich (1979) and is described thereby in detail and also in Sofue (1982). With this technique we can abstract structures with angular scale sizes smaller than a certain beamwidth by filtering out larger-scale structures than the beamwidth. The method is useful to search for low-brightness and small-scale (compared with the filtering beamwidth) objects that are hidden or merged in a strong background radio emission with steep intensity gradient like that due to the galactic disk component.

2.2 RESULTS. — The resulting maps are displayed in figures 1 and 2 in the form of contour maps. We take a Gaussian filtering beam with a full width of $\Theta = 4°$. The spatial resolution of the maps is limited by the original beamwidth of the telescopes : HPBW for the 408 MHz Bonn survey is 0°.6, that for the Jodrell survey is 1° and that for the 820 MHz Leiden survey is 1°.5.

A number of structures of various kinds are found in the figures. In figure 3 we compare the 408 MHz map with known HI shells and some other objects. HI shells of

Heiles (1979) and Hu (1981) are marked with thin, full lines, except for a few marked with thick lines which are positionally in coincidence with radio loops. Some loop structures associated with HI shells in the data of Colomb *et al.* (1980) are indicated with thick dashed lines, which are discussed in detail in the next section. Filled circles are positions of SNRs catalogued by Milne (1979). Crosses in figure 3 show positions of pulsars (Manchester and Taylor, 1981). As seen from the figure, it is rather striking that most of the Heiles' and Hu's HI shells are not associated with radio continuum loops with only a few exceptions. We also find that there is no significant correlation of the HI shells and/or radio loops with pulsars.

In the following we discuss some typical radio features noticed in figures 1-3. For later convenience we denote a radio loop as G28 + 32 D12, which means a galactic radio loop located at $l = 28°$, $b = 32°$ and with the diameter of approximately 12°.

The North Polar Spur : The feature is most remarkable among the other structures. The NPS ridge emerges from $l = 25°$, $b = 8°$ and extends toward high galactic latitudes, drawing a giant arc on the sky. The spur is composed of many thin ridges at $b = 30$-$60°$. Figure 4a demonstrates the fine structures of the North Polar Spur in its full extent in the Bonn survey. The figure was obtained with the same method as that used in obtaining figures 1-3, but displayed in a grey scale so that the distribution of the ridges are more clearly recognized.

Radio loop G28 + 32 D12 : The loop is centered on $l = 28°$, $b = 32°$ and elongated in the north-south direction. The loop is superposed on the ridge of the NPS, and may be a substructure of the NPS. The loop is recognized as well on the 820 MHz map. This object is enlarged in figure 4b.

Arc complexes at $30° < l < 60°$, $-20° < b < 20°$: Many fragmentary arc structures are found at $30° < l < 60°$, $-20° < b < 20°$. Some of them are recognized as parts of loop-structures, which are discussed below (G40 − 07D 05, G41 + 21 D10, G56 + 14 D10), while others are difficult to be recognized as systematic structures. The latter may be caused by fluctuations of the radio emission like background as due to the turbulent interstellar magnetic fields and distribution of cosmic rays. We enlarge this region at 408 MHz in figure 4c, where the structures are displayed in grey scale.

G40 − 07 D05 : This composes an arc in the farther side of the galactic plane extending along more than a half way of a loop centered on $l = 40°$, $b = 7°$ with the diameter of approximately 5° (see fig. 4c). This structure is cleary recognized both in the 408 MHz and 820 MHz maps. The loop is elongated slightly in the direction of latitude. In spite of our search, the loop is not associated with any HI feature.

G56 + 14 D10 : This loop has been reported by Sofue (1982) in detail. The loop is associated with an HI shell (dashed line in fig. 4d) at radial velocity of 25 km/s (LSR), which puts the loop at a kinematical distance of 1.9 kpc and the linear diameter is estimated to be approximately 300 pc. This may be one of the oldest SNRs in the solar neighbourhood, located high above the galactic plane ($z \sim 0.5$ kpc). It may be in a very late stage of SNR evolution, just before loosing its identity.

G88 − 13 D9 : This is associated with an HI shell of radial velocity $-15 \sim +7$ km/s (Hu's shell No. 9), and will be a very local structure. The western ridge of the loop at $l = 85°$, $b = -10°$ is apparently associated with diffuse optical filaments which are found on the Palomar Sky Survey E(red) print. In figure 4g we enlarge this loop and indicate the optical filaments with shaded area.

G117 − 07 D7 : This arc-shaped ridge of radio enhancement in the 820 MHz map (the 408 MHz map is lacking) composes a part of a loop centered on $l = 117°$, $b = -7°$ and its diameter is approximately 7°. This loop is positionally in coincidence with the Heiles HI shell GS117-07-67 (dashed line in fig. 4f ; see sect. 7).

G209 + 00 D7 : This loop is centered on $l = 209°$, $b = 0°$ with the diameter of 7° (Fig. 4g). Its northern side is a part of the Monoceros loop centered on $l = 207°$, $b = 1°$ with the diameter of 3°. The Rosetta Nebula ($l = 207°$, $b = -2°$) is just on the western edge of this loop.

3. Association with HI shells.

We examine the association of HI gas features with the radio loops and *vice versa* by comparing our maps with the HI line data of shells and supershells of Heiles (1979) and Hu (1981) together with the HI maps presented by Colomb *et al.* (1980). Table I lists radio continuum loops at 408 MHz which are apparently associated with HI shell-like features. The table gives their characteristic parameters like their sizes, brightness, diameters, distances and HI radial velocities. The loops are divided into two classes : Class A for those with higher certainty, which are recognized clearly as loops, and Class B for those with less certainty mostly recognized as fragmentary enhancements in radio brightness oriented along loops defined by the HI shell ridges. Among the loops, G88-13 and G203 + 17 are identified with the Hu's HI shells No. 9 and 29, respectively. Loop G117 − 07 coincides positionally with a Heiles stationary shell GS117-07-67.

In the following we describe the quantities given in table I in the order of the columns.

Column 1 : The class and serial number of the loop in each class.

Column 2 : Designation of the loop, indicating its galactic longitude and latitude. The error in the position determination is approximately ± 1°.

Column 3 : Apparent size on the sky, separately given in the directions along the latitude and longitude, respectively. The error is approximately ± 1°.

Column 4 : Mean brightness temperature averaged over the loop extent at 408 MHz. The error in the temperature is approximately ± 50 % for 408 MHz data.

Column 5 : Mean surface brightness given through $\Sigma = 2\,\nu^2 k T_b/c^2$ where ν is the frequency, k is the Boltzmann constant and c is the light velocity. The error in Σ is the same as in T_b.

Column 6 : The surface brightness at 1 GHz estimated from 408 MHz brightness by assuming a spectral index of $\alpha = -0.6$.

Columns 7-12 : The parameters of the radio loop, when it is assumed to be a normal supernova remnant. The quantities are obtained by applying the surface brightness-diameter (Σ-D) relation of Milne (1979) to the mean surface brightness at 1 GHz in Column 6 and the apparent angular sizes in Column 3.

Column 7 : The diameter D is related to the surface brightness at 1 GHz through

$$D(\mathrm{pc}) = 4.12 \times 10^{-4} \Sigma^{-0.25} \exp(-|z|/214\ \mathrm{pc}) .$$

The error in D is estimated through

$$\delta D/D = \{(0.25\,\delta\Sigma/\Sigma)^2 + (\delta|z|/214)^2\}^{1/2} .$$

Combining $\delta\Sigma/\Sigma \sim 0.5$ with the error in z obtained in the following column, we have $\delta D/D \sim 0.2$. However, as the Σ-D relation itself should have intrinsically larger error of the order of a factor unity, we must take the error in D as $\delta D/D \sim {}^{+1}_{-0.5}$.

Column 8 : The height of the center of the loop above the galactic plane is given through

$$z = D.\ \sin b/\Delta b .$$

If we recall that $\delta D/D \sim {}^{+1}_{-0.5}$, the error in z will be $\delta z/z \sim {}^{+1}_{-0.5}$.

Columns 9 and 10 : Distance of the loop center from the sun, d, and its projected distance on the galactic plane. The error in d is of the order of $\delta d/d \sim {}^{+1}_{-0.5}$.

Column 11 : Initial explosion energy of an SNR is estimated through

$$E_0 = 5.3 \times 10^{43}\, n_0^{1.12} (D/2)^{3.12}\, v^{1.4}\ \mathrm{ergs} ,$$

which has been derived by Chevalier (1974) for an expanding shell with the diameter D (in pc) at an expansion velocity of v (km s^{-1}) in an interstellar medium of number density n_0 (cm^{-3}). We assume $v = 10$ km s^{-1} and $n_0 = 1$ cm^{-3}.

Column 12 : The age of the SNR given through $t = 3/2\ D/v.10^5$ years with D in pc and v in km s^{-1}. Parameters for the associated HI shells are given in Columns 13 to 19. Except for Loop No A-2, B-8, and A-3 which are identified with Hu's (1981) or Heiles' (1979) shells, the quantities are obtained from the HI survey data of Colomb *et al.* (1980). Those for No. A-2, A-3 and B-8 are taken from Hu (1981) and Heiles (1979).

Column 13 : The position of the center of the HI shell in the galactic coordinates. The error in position is approximately ± 2°.

Column 14 : Apparent extents in the latitude and longitude directions. The error is approximately ± 2°.

Column 15 : Minimum and maximum radial velocities of the shell and center radial velocity. The error is approximately ± 4 km s^{-1}.

Columns 16 and 17 : Distance of the shell using the center velocity in Column 15 except for Hu's shells. A circular rotation of the Galaxy was assumed following Schmidt (1966). The error is typically about 20 %. The projected distance on the galactic plane is also given. Distances to Hu's shells are taken from his paper.

Column 18 : Linear extents in the latitude and longitude directions, which are evaluated from the distance in Column 16 and the apparent extents in Column 14. The error is typically about 30 %.

Column 19 : Height from the galactic plane of the shell center.

Column 20 : Identification with the HI shells in Hu (1981) and Heiles (1979).

We find that the distances derived from the Σ-D relation are generally smaller than those derived from the kinematic relation. Distances derived by Hu's (1981) method are generally smaller than those derived using the Σ-D relation. However, in some cases like Loops No. A-2, B-6, B-8 and B-9, the distances from the Σ-D relation agree with the HI distances within the range of the error. In these cases it is reasonable to judge that the radio continuum loops are physically associated with the HI shells. In particular the two distances for the lop B-9 are in good agreement with each other. The angular extent of the radio loop B-9 is also in good agreement with that of its HI shell. In other cases the association of the radio continuum loop with the HI shells is rather unclear, for which the Σ-D and HI distances disagree with each other.

4. Discussion.

4.1 EXTREMELY OLD SNRS HIGH ABOVE THE GALACTIC PLANE. — We have searched for radio continuum loops of medium size between 3 and 15 degrees in diameter. Among many loop-like features, nine of them are possibly associated with HI shells of the same diameters. From the distance estimates of the radio loops and HI shell, five loops are likely to be physically associated with HI shells. They are G88 − 13, G104 − 18, G203 + 17 and G232 + 11. If these loops are assumed to be SNRs, their ages are of the order of 10^6 years and may be extremely old SNRs just before loosing their identity by merging into the interstellar medium. Their distances from the sun are between 0.3 and 1.2 kpc and are located high above the galactic plane, or at $|z| \geq 200$ pc.

We estimate an expected number $N(t, z, d)$, of SNRs with ages less than or equal to t in the solar vicinity and located higher above the galactic plane than $|z|$ and distances less than d. Let the rate of SN explosion in our Galaxy be f, then the expected number is given through

$$N(t, z, d) = \pi d^2 f t\, \gamma(R) \exp(-|z|/100\ \mathrm{pc}) ,$$

where $\gamma(R)$ is a fractional surface density of SNRs projected on the galactic plane at a galactocentric distance R, and a z-dependence of SNR density in the form of exp $(-|z|/100$ pc) (Sofue, 1982) is assumed. Since the SN rate is proportional to the star formation rate and the star formation rate is proportional to the square of gas density σ_g (e.g., Hamajima and Tosa, 1974 ; Nakai and Sofue, 1982), we have

$$\gamma(R) = \sigma_g^2(R) / \int_0^\infty \sigma(r)^2\, 2\,\pi r\, \mathrm{d}r .$$

We adopt a density distribution of molecular hydrogen gas given by Gordon and Burton (1976) as $\sigma_g(R)$ and obtain

$$N(t, z, d) = \pi d^2 f t \, [\sigma_g(R)/\sigma_g(R_\odot)]^2/(1\,400 \text{ kpc}^2) \exp(-|z|/100 \text{ pc}) .$$

Taking a SN rate, f = one per 30 years (e.g. Milne, 1979), we obtain the expected number of SNRs at $R = 10$ kpc with ages $t = 10^6$ years located at $d \leqslant 1$ kpc and $|z| \geqslant 200$ pc as

$$N(t \leqslant 10^6 \text{ y}, |z| \geqslant 200 \text{ pc}, d \leqslant 1 \text{ kpc}) \sim 10.1.$$

Since the coverage of the sky in our search is from $l = 30°$ through $l = 240°$, the expected number of such SNRs in our coverage is approximately six, which is close to that found in section 4. It will be therefore reasonable to conclude that almost all extremely old SNRs in the solar vicinity have been picked up in the present search.

4.2 ABSENCE OF ASSOCIATION OF RADIO LOOPS WITH HEILES' AND HU'S HI SHELLS. — The majority of the HI shells and supershells of Heiles (1979) and Hu (1981) are not associated with radio continuum emission. This fact confirms the Heiles' conclusion : radio continuum emission of such large-diameter shells will be extremely difficult to detect, if the shells follow the usual surface brightness-diameter relationship of SNRs. This conclusion is particularly true for HI shells found at low galactic latitudes, $|b| < 10°$, where the galactic background emission is so strong that even the BGF method is less powerful compared with « quiet » region at higher latitudes.

However, the absence of association with Hu's HI shells, which are located at higher latitudes poses a puzzling problem on their origin except for a few given in table I : if they follow the surface brightness-diameter relationship of SNR, they should certainly be detected by our survey. This suggests that Hu's shells are much less energetic phenomena than usual supernova remnants. Indeed kinetic energy of Hu's shells is of the order of 10^{48} ergs (Hu, 1981), two to three orders of magnitude smaller than that of usual SNRs.

4.3 RELATION TO THE GALACTIC RADIO LOOPS. — Four giant radio continuum loops, Loop I-IV, are known so far and discussed by many authors (e.g., Berkhuijsen *et al.*, 1971). In our analysis of the 408 MHz and 820 MHz radio continuum data Loop I (NPS) is clearly recognized as composed of giant arcs in figures 1 and 2, while Loop II and III are not found in our figures.

Loop I is an ensemble of many bright, thin ridges with thickness less than 4° superposed on larger scale structures as seen on the original 408 and 820 MHz maps of Haslam *et al.* (1974) and Berkhuijsen (1972). On the other hand Loop II and III are very diffuse and have no such thin, bright ridges in spite of their smaller angular diameters than Loop I. This large difference in their structures suggests that Loop II and III are phenomena quite different from Loop I. In this respect readers may refer to Sofue (1976), who argues that Loops II and III are galactic scale structures connected to the spiral arms.

If we stand on the SNR hypothesis of Loop I-IV, a question may arise : why loop structures of medium size between the four loops of diameters greater than 40° and known SNRs of diameters mostly less than ~ 3° are not found as yet (Sofue *et al.*, 1974). The radio loops found in the present paper are likely to be such medium-size nearby SNRs filling the gap.

References

BERKHUIJSEN, E. M. : 1972, *Astron. Astrophys. Suppl. Ser.* **5**, 263.
BERKHUIJSEN, E. M., HASLAM, C. G. T., SALTER, C. J. : 1971, *Astron. Astrophys.* **14**, 252.
CHEVALIER, R. A. : 1974, *Astrophys. J.* **188**, 501.
COLOMB, F. R., POPPEL, W. G. L., HEILES, C. : 1980, *Astron. Astrophys. Suppl. Ser.* **40**, 47.
GORDON, M. A., BURTON, W. B. : 1976, *Astrophys. J.* **208**, 346.
HAMAJIMA, K., TOSA, M. : 1975, *Publ. Astron. Soc. Jpn.* **27**, 561.
HASLAM, C. G. T., QUIGLEY, M. J. S., SALTER, C. J. : 1970, *Mon. Not. R. Astron. Soc.* **147**, 405.
HASLAM, C. G. T., WILSON, W. E., GRAHAM, D. A., HUNT, G. C. : 1974, *Astron. Astrophys. Suppl. Ser.* **13**, 359.
HEILES, C. : 1979, *Astrophys. J.* **229**, 533.
HEILES, C., JENKINS, E. B. : 1976, *Astron. Astrophys.* **46**, 333.
HU, E. M. : 1981, *Astrophys. J.* **248**, 119.
MANCHESTER, R. N., TAYLOR, J. H. : 1981, *Astron. J.* **86**, 1959.
MILNE, D. K. : 1979, *Aust. J. Phys.* **32**, 83.
NAKAI, N., SOFUE, Y. : 1982, *Publ. Astron. Soc. Jpn.* **34**, 199.
SCHMIDT, M. : 1966, in *Galactic Structure, Stars and Stellar Systems V*, eds A. Blaauw, M. Schmidt (Univ. Chicago Press) p. 513.
SOFUE, Y. : 1976, *Astron. Astrophys.* **48**, 1.
SOFUE, Y. : 1983, *Publ. Astron. Soc. Jpn.* **35**, 91.
SOFUE, Y., HAMAJIMA, K., FUJIMOTO, M. : 1974, *Publ. Astron. Soc. Jpn.* **26**, 399.
SOFUE, Y., REICH, W. : 1979, *Astron. Astrophys. Suppl. Ser.* **38**, 251.

TABLE I. — *Radio loops and associated HI shells (see the text as to the legend).*

Radio Loop												HI shell							
Class-No.	Designation	Angular size	T_b(°K)	Σ(Wm^{-2} Hz^{-1} str^{-1})		D	Z	d	d cos b	E_0	t	position	size	LSR velocity (km/s)		d	d cos b	size	z=d sin b	Heiles/Hu
	(1° b°)	Δl cos b x Δb	408MHz	408MHz	1 GHz	(pc)	(pc)	(pc)	(pc)	(ergs)	(yr)	1° b°	Δl cos b°x Δb°	V_{min} -V_{max}	V_{center}	(pc)	(pc)	(pc)	(pc)	No.
(1)	(2)	(3)	(4)	(5)		(6)	(7)	(8)	(9)	(10)	(11)	(12)	(13)	(14)	(15)		(16)	(17)	(18)	(19)	(20)
A - 1	G 56 + 14	10° x 10°	1.0	$5.1\cdot10^{23}$		$3.0\cdot10^{23}$	95x95	130	540	520	$2.3\cdot10^{50}$	$1.4\cdot10^{6}$	55°+ 15°	10° x 11°	+ 8 ~ +34	+25	1.9×10^{3}	1.8×10^{4}	330x360	490	-
A - 2	G 88 - 13	7 x 7	0.5	2.6		1.5	94x94	-170	770	750	2.2	1.4	88°- 13°	9° x 7°	-15 ~ + 7	0	410	400	50	92	Hu - 9
A - 3	G117 - 07	6 x 7	-	-		1.8	110x120	-110	900	890	4.1	1.7	117°- 07°	7° x 8°	-71 ~ -63	-67	6.3×10^{3}	6.3×10^{3}	410	770	Heiles GS117-07-67
B - 1	G 57 + 41	10 x 16	0.1	0.5		0.3	79x102	270	410	310	1.9	1.4	55°+ 42°	10° x 14°	- 8 ~ + 0	- 4	-	-	-	-	-
B - 2	G 65 + 16	12 x 9	0.2	1.0		0.6	123x108	180	650	630	4.2	1.7	66°+ 15°	10° x 10°	-17 ~ + 4	- 4	-	-	-	-	-
B - 3	G 75 - 16	8 x 7	0.2	1.0		0.6	102x96	-210	760	730	2.6	1.5	75°- 15°	9° x 9°	- 4 ~ + 4	0	-	-	-	-	-
B - 4	G 80 - 22	7 x 8	0.4	2.0		1.2	75x81	-220	590	540	1.2	1.2	80°- 20°	7° x 7°	0 ~ + 8	+ 4	-	-	-	-	-
B - 5	G 98 - 27	7 x 6	0.4	2.0		1.2	68x62	-260	570	510	0.7	1.0	99°- 26°	7° x 8°	-34 ~ -21	-25	3.5×10^{3}	3.1×10^{4}	430x490	1530	-
B - 6	G104 - 18	9 x 9	0.5	2.6		1.5	91x91	-180	580	550	2.0	1.4	104°- 18°	9° x 8°	-13 ~ - 4	- 8	1.0×10^{3}	1.0×10^{3}	160x140	310	-
B - 7	G176 - 16	5 x 6	0.2	1.0		0.6	80x89	-240	870	840	1.6	1.3	175°- 15°	6° x 6°	-21 ~ - 8	-17	-	-	-	-	-
B - 8	G203 + 17	4 x 4	0.2	1.0		0.6	69x69	290	990	950	0.8	1.0	203°+ 17°	5°5 x 4°	-11 ~ + 5	- 1	405	387	33	118	Hu - 29
B - 9	G232 + 11	3 x 2	0.4	2.0		1.2	69x55	280	1470	1440	0.6	0.9	231°+ 11°	3° x 2°	+13 ~ +21	+17	1.2×10^{3}	1.2×10^{3}	60x40	230	-

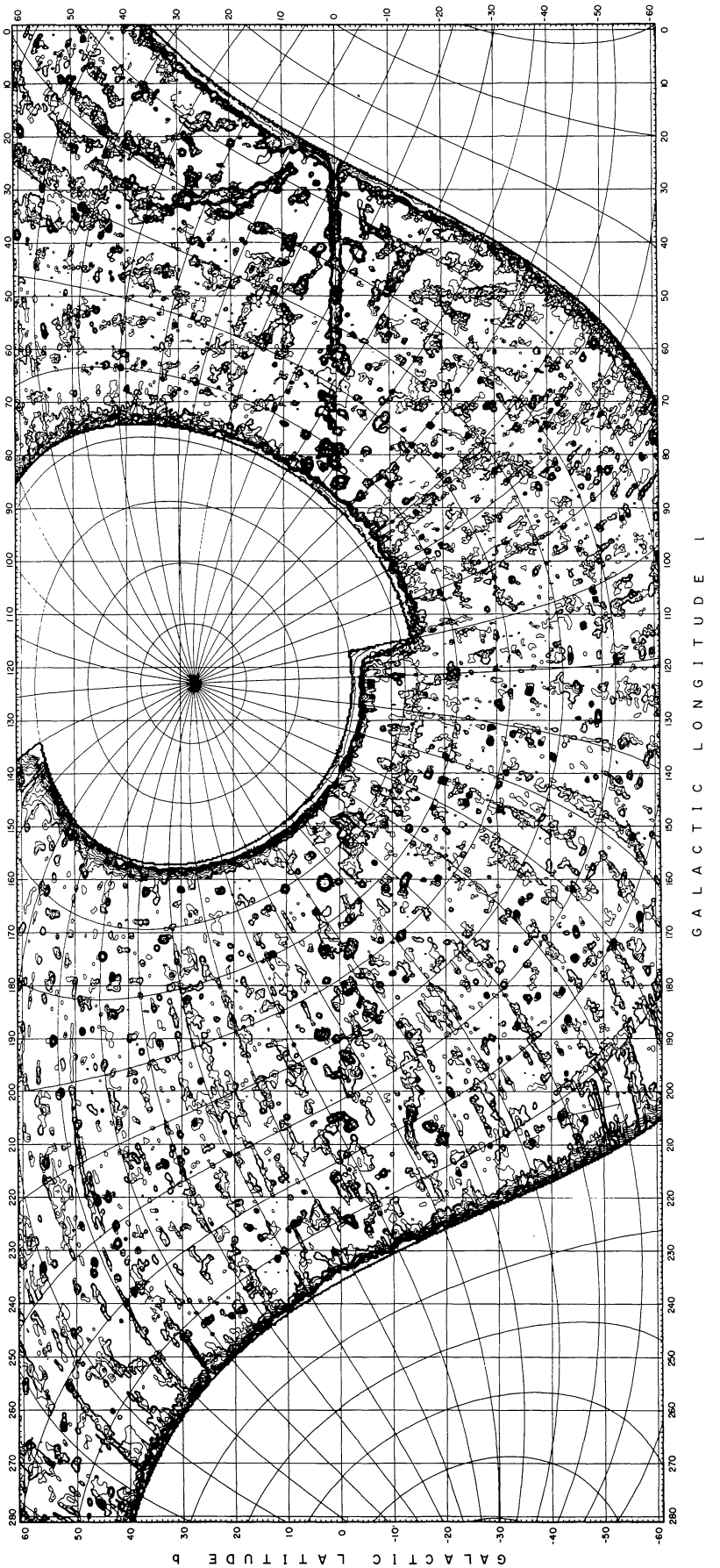

FIGURE 1. — 408 MHz T_b map showing structures with scale sizes smaller than 4°. The background filtering (BGF) method has been applied to the Jodrell Bank (Haslam *et al.*, 1970 ; RA = 0-12^h) and Bonn surveys (Haslam *et al.*, 1974 ; RA = 12-24^h). The lowest contours are at T_b^{408} = 0.5 K. Then the contour levels are in step 1 K from T_b = 1 K through 10 K, in step 10 K from 10 through 100 K, in step 100 K from 100 through 1 000 K and in step 1 000 K above T_b = 1 000 K.

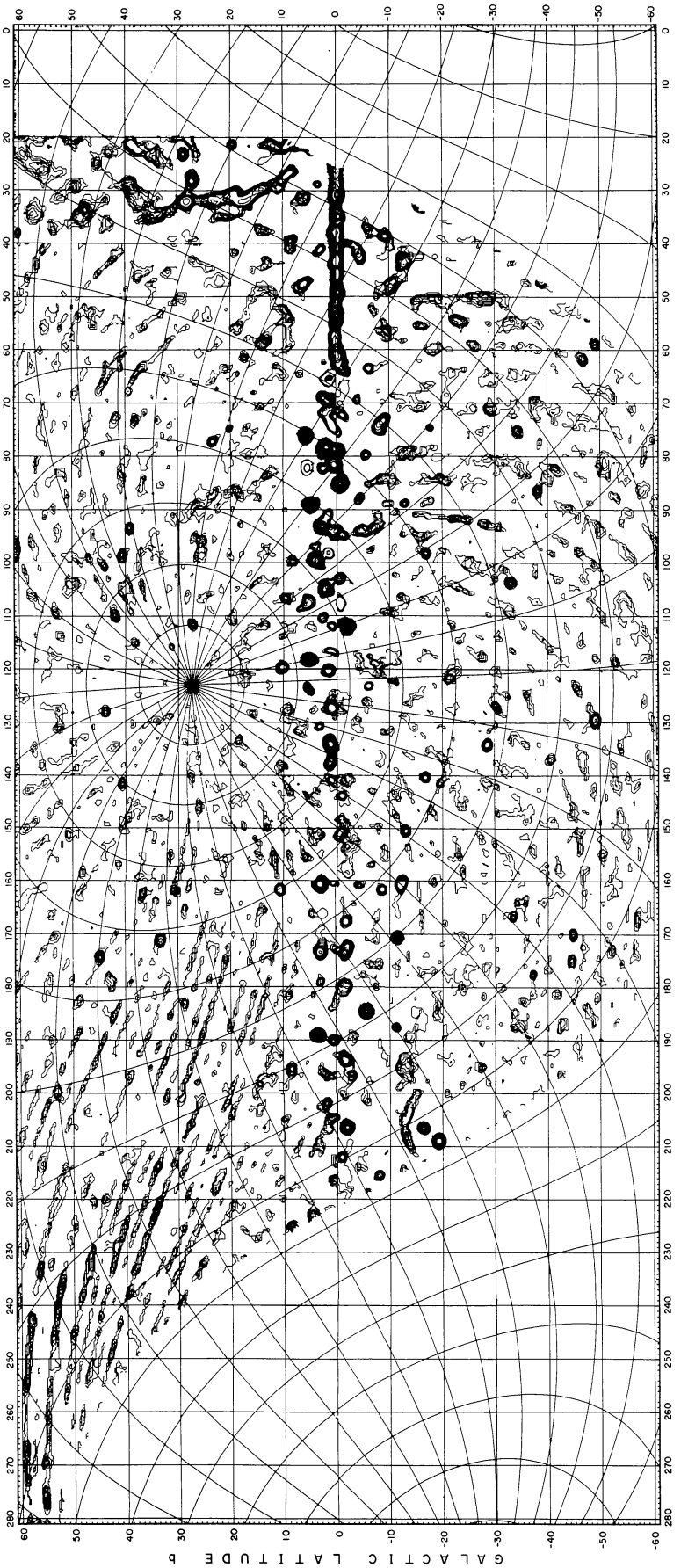

FIGURE 2. — 820 MHz T_b map showing smaller structures than scale sizes of 4°. BGF has been applied to the Leiden survey (Berkhuijsen, 1972). The contour levels are T_b^{820} in step 0.1 K from T_b = 0.1 through 1 K in step 0.5 K from 1 through 10 K, in step 5 K from 10 K through 100 K, and in step 50 K above 100 K.

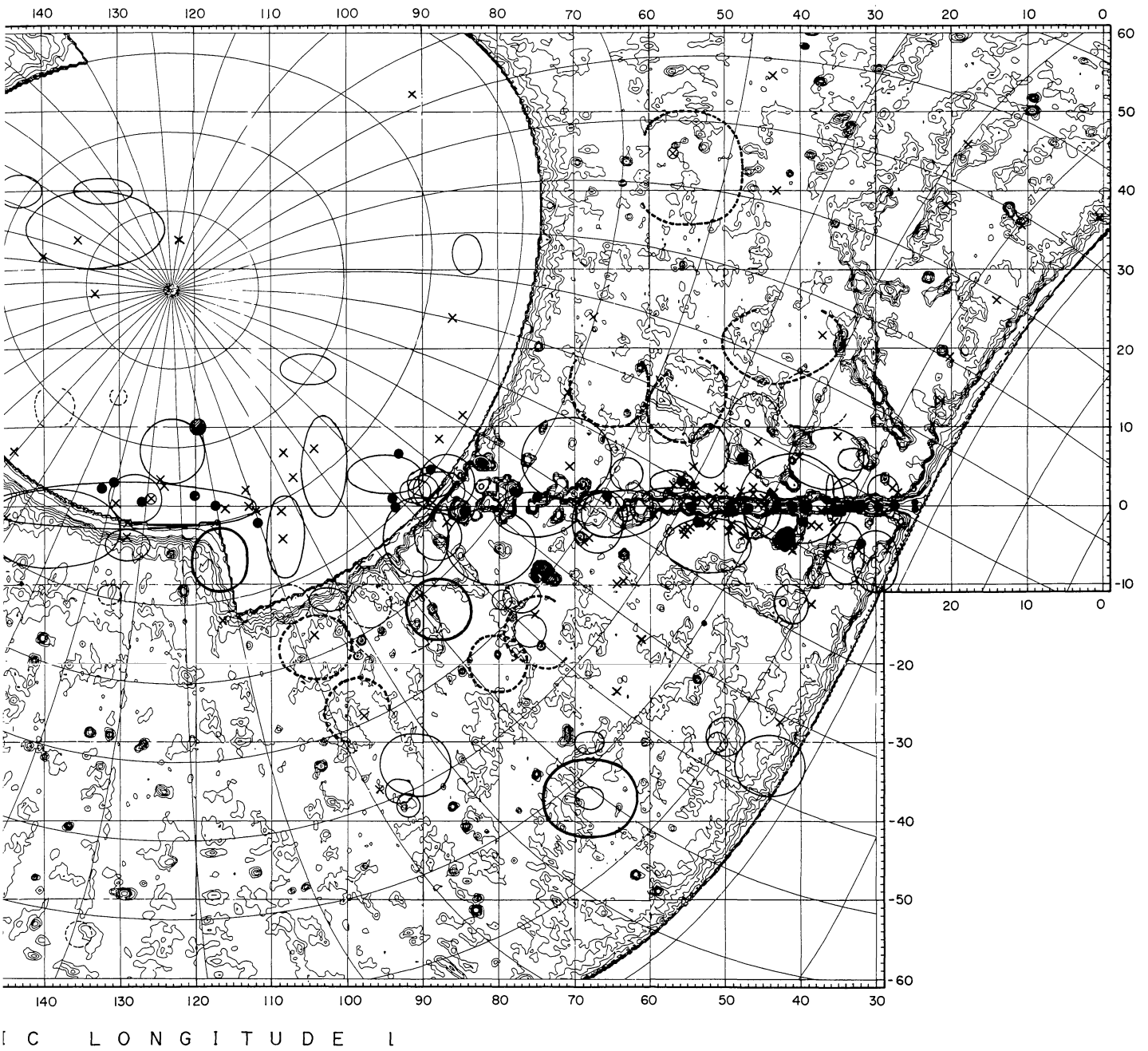

re at T_b^{408} = 5 K. Then the contour levels are in step 20 K from
00 K, in step 200 K from 200 K through 1 000 K, in step 1 000 K from
)0 K. HI shells of Heiles (1979) and Hu (1981) are shown by thin-line
y thick-line ellipses. Newly found HI shells associated with radio loops
Rs and crosses are positions of pulsars.

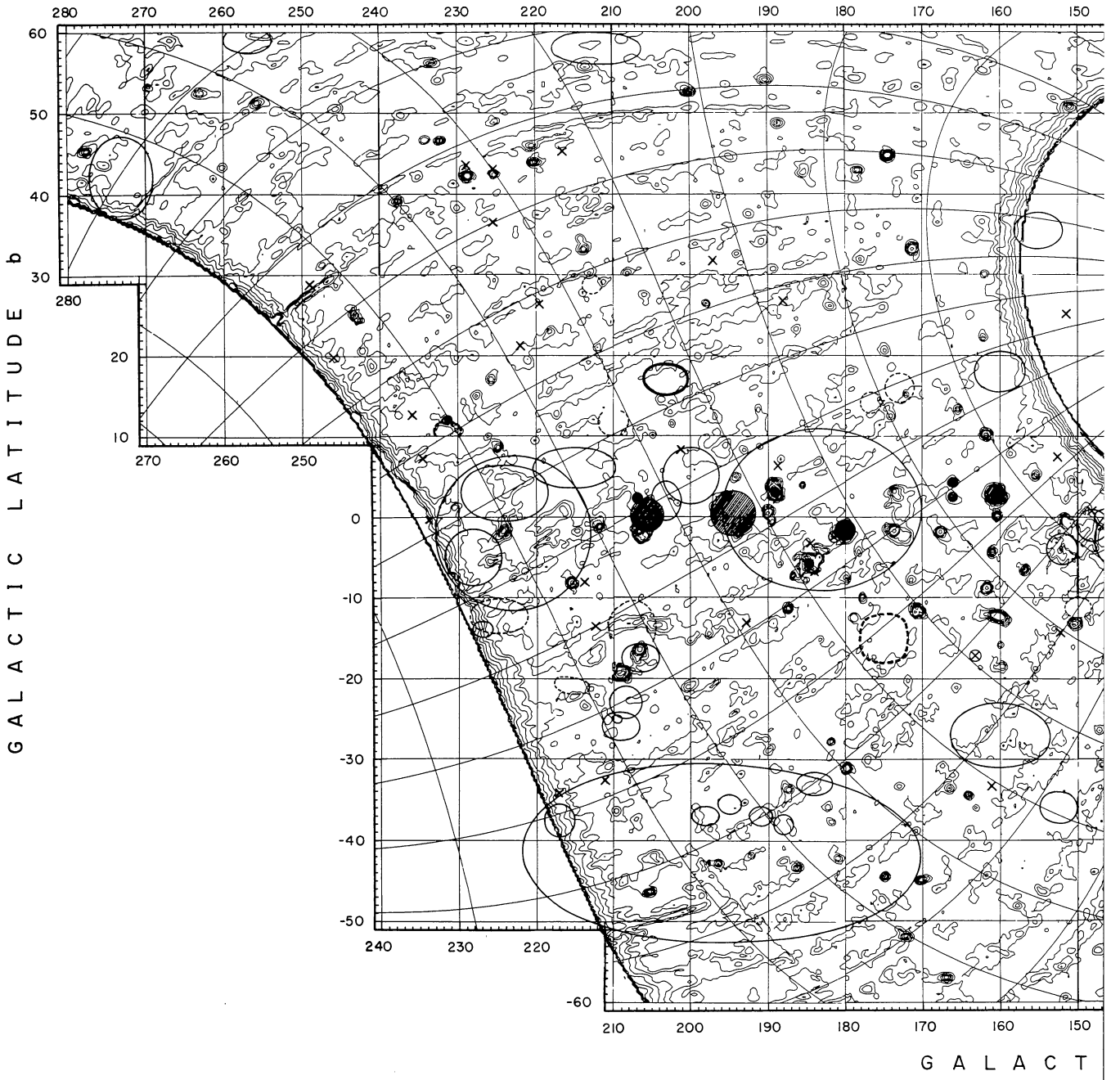

FIGURE 3. — The same as fig. 1, but the lowest contours
T_b = 20 K through 100 K, in step 100 K from 100 K through
1 000 K through 2 000 K, and in step 2 000 K above T_b = 2
ellipses, and those associated with radio continuum loops are
are indicated with dashed lines. Hatched circles are known S

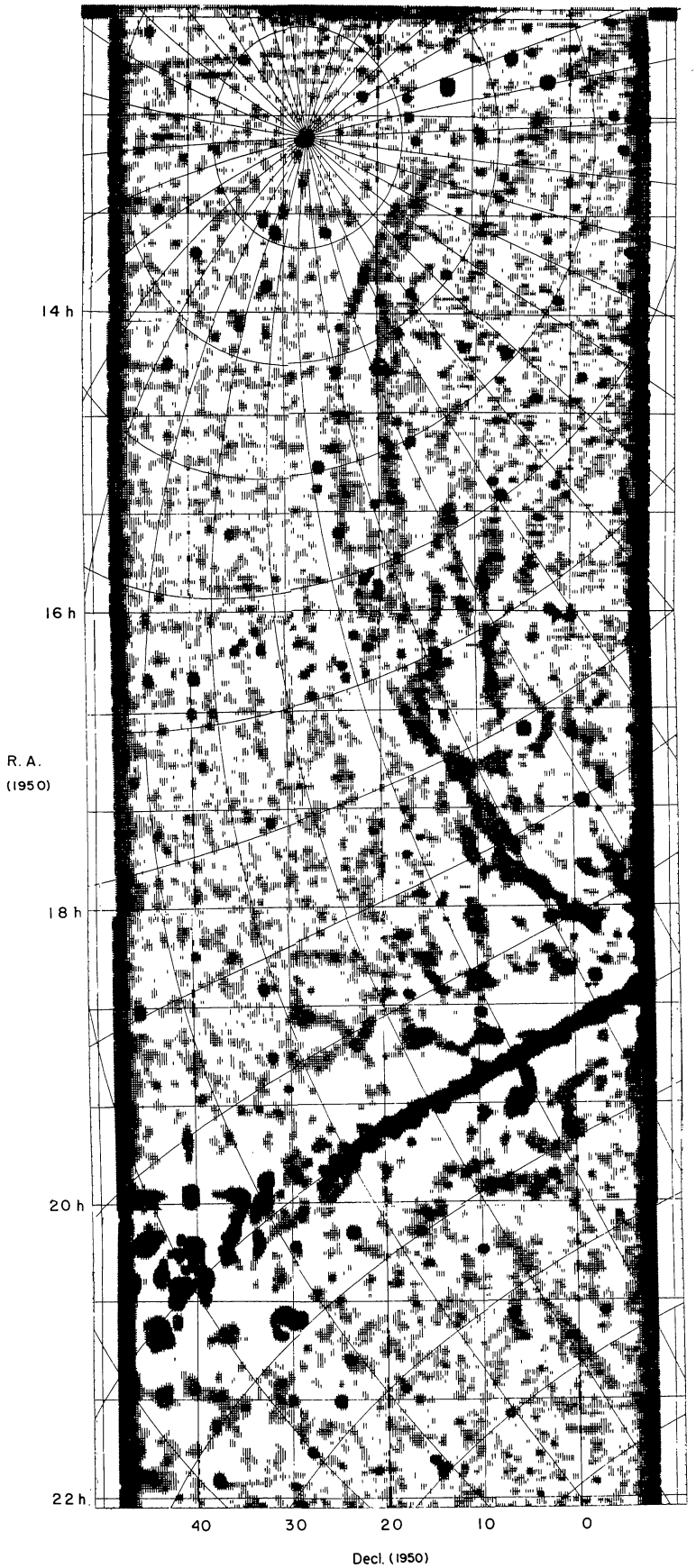

FIGURE 4a.

FIGURE 4. — Some typical radio loops found in figs. 1 and 2. Figs. 4a through 4c show the 408 MHz T_b distributions displayed in grey scale, where regions of T_b from 5 K through 20 K are hatched, regions of 20 K through 200 K are cross hatched, and above are dark. Figs. 4d through 4g are enlarged from figs. 1 and 2, where the contour levels are the same as in figs. 1 and 2.

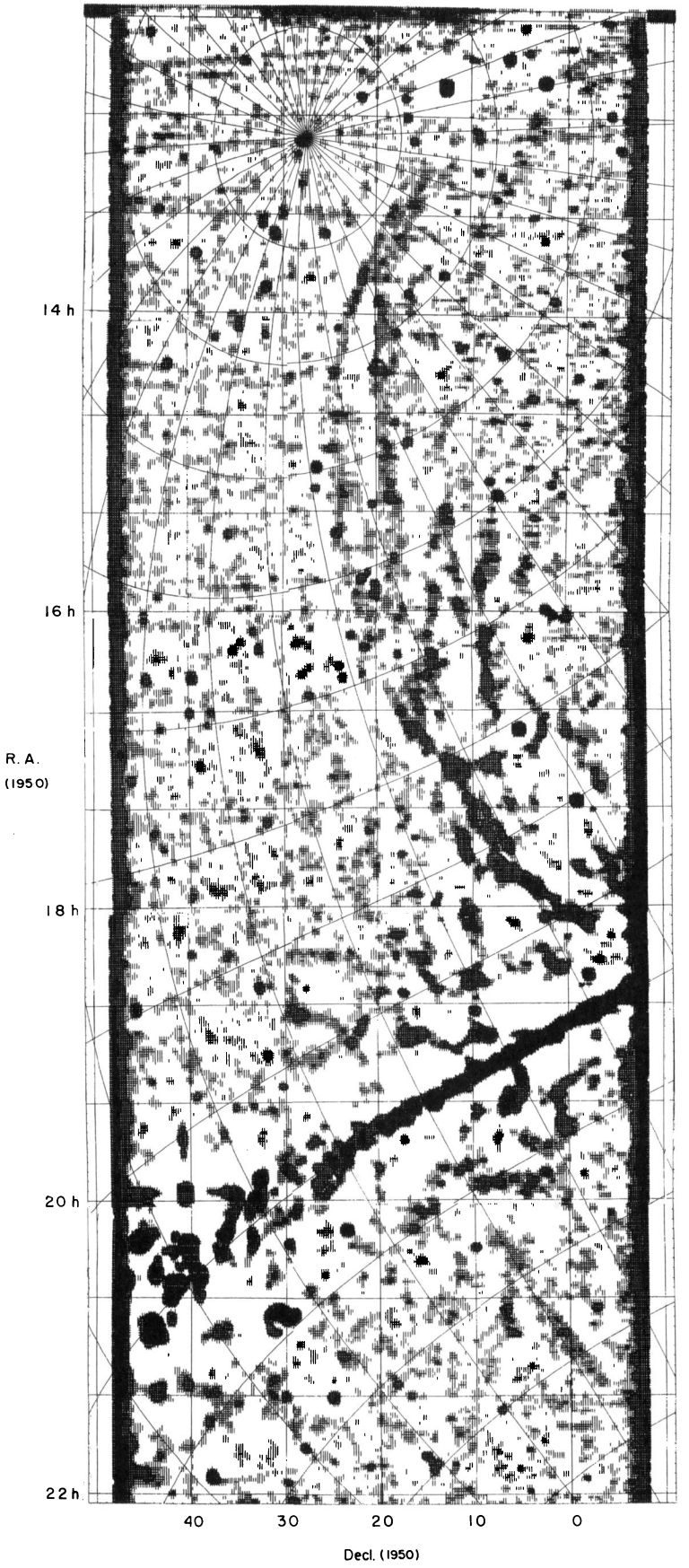

FIGURE 4a.

FIGURE 4. — Some typical radio loops found in figs. 1 and 2. Figs. 4a through 4c show the 408 MHz T_b distributions displayed in grey scale, where regions of T_b from 5 K through 20 K are hatched, regions of 20 K through 200 K are cross hatched, and above are dark. Figs. 4d through 4g are enlarged from figs. 1 and 2, where the contour levels are the same as in figs. 1 and 2.

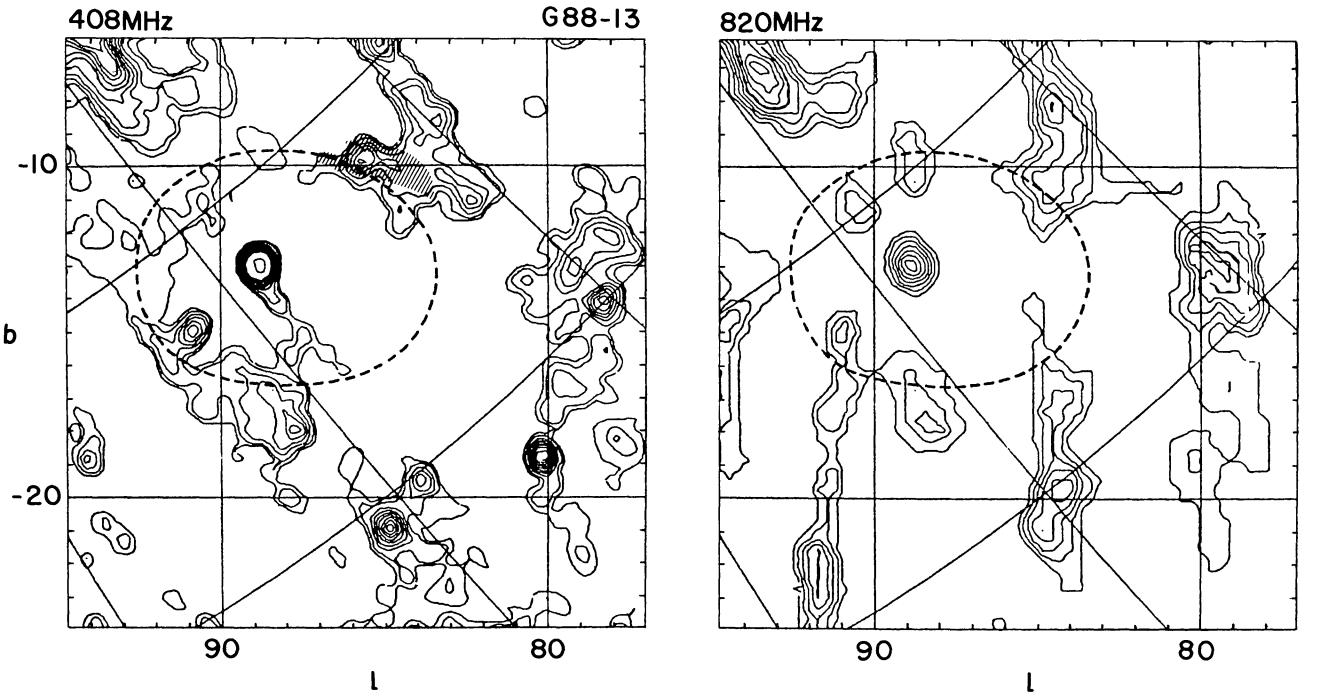

FIGURE 4e.

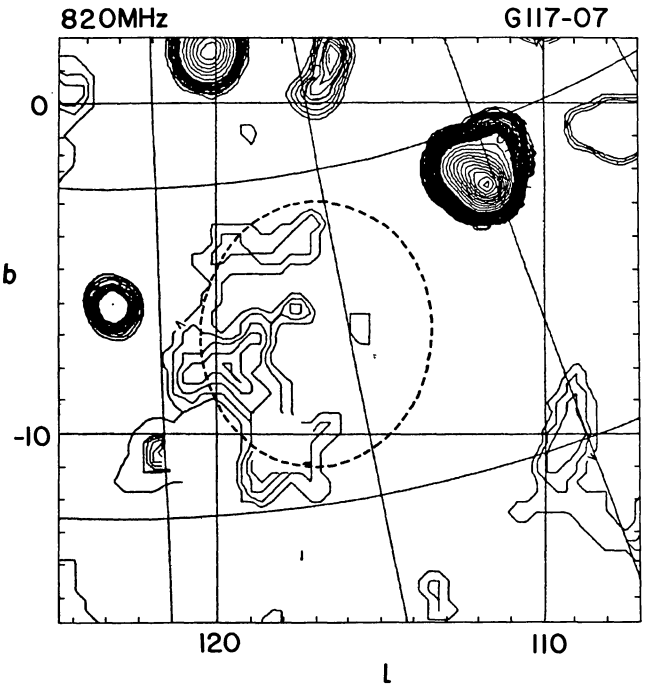

FIGURE 4f.

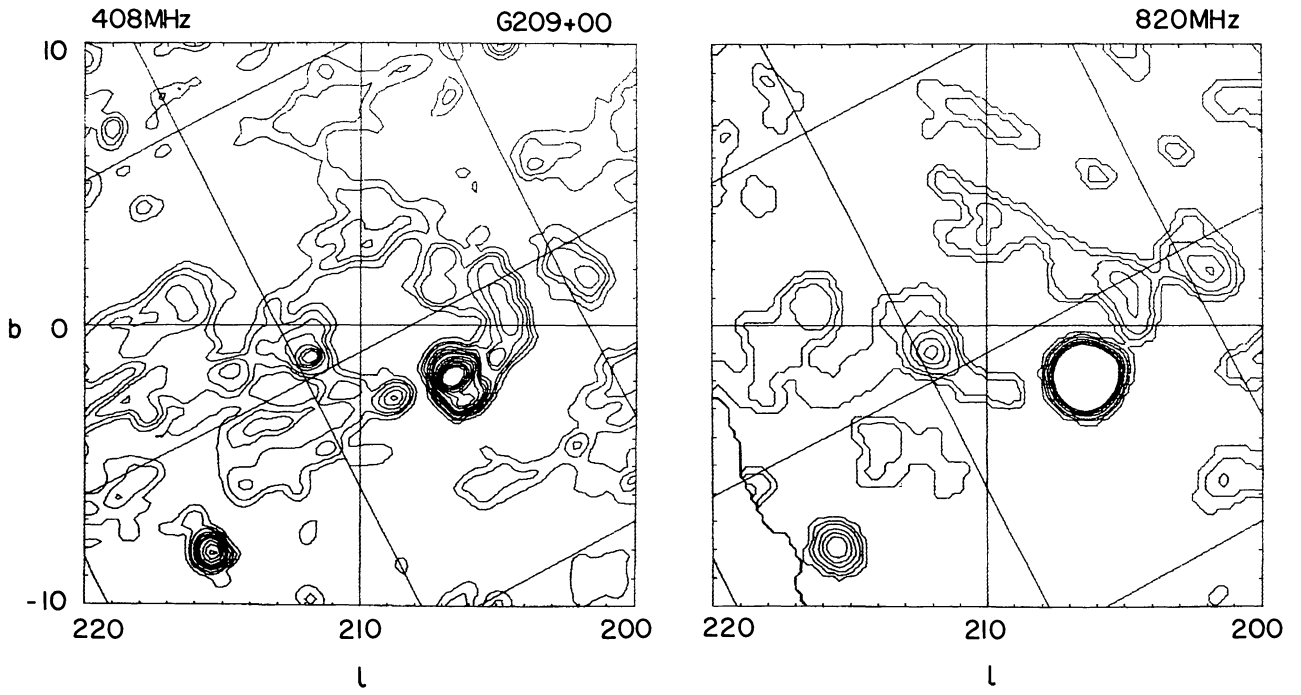

FIGURE 4g.

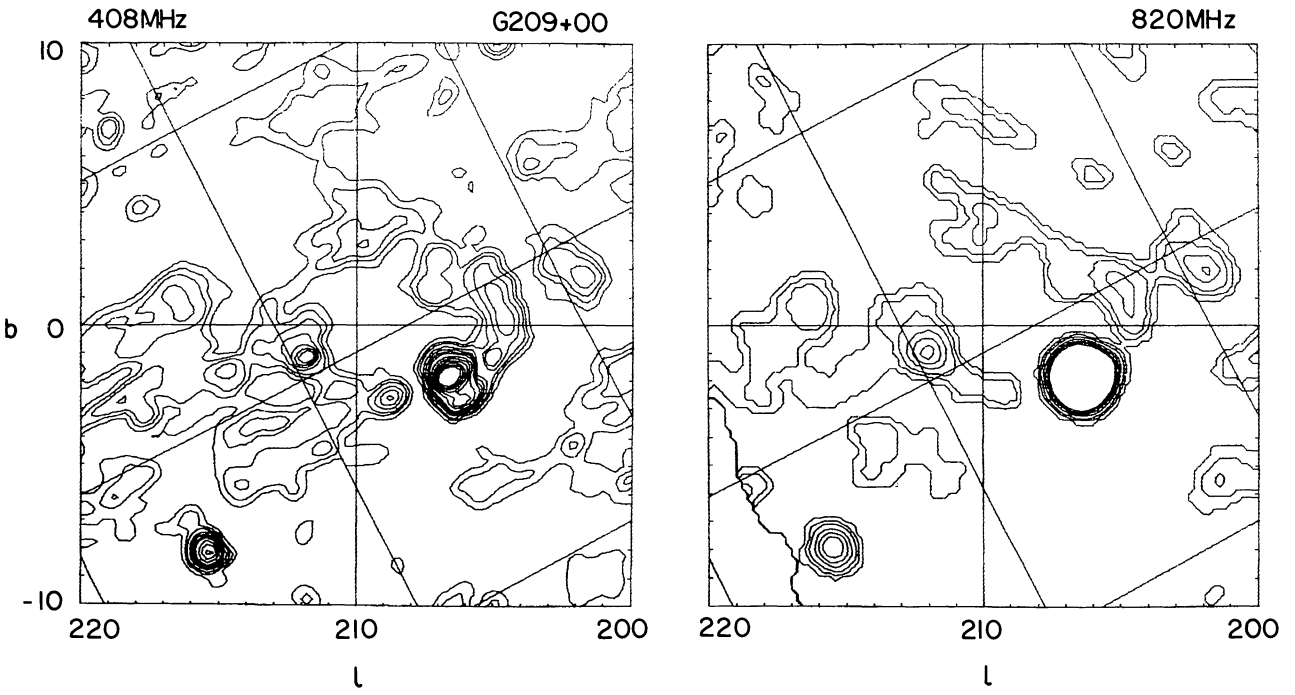

FIGURE 4g.